Chapter 4
Photonic DNA Nano-Processor: A Photonics-Based Approach to Molecular Processing Mediated by DNA

Yusuke Ogura, Takahiro Nishimura, Hirotsugu Yamamoto, Kenji Yamada and Jun Tanida

Abstract This chapter describes a photonic deoxyribonucleic acid (DNA) nano-processor, which is capable of dealing with molecules as real objects and with their associated information simultaneously in a bio-molecular environment. We present a light-activatable DNA nano-processor and DNA scaffold logic as implementation methods, and reveal their fundamental properties through experimental and analytical results.

4.1 Introduction

The importance of methods for observation and control of molecular events is increasing in a variety of fields, including life sciences and environmental technology. For example, molecular imaging, which enables us to visualize the activities of various bio-molecules, is helpful in understanding vital functions on a molecular

Y. Ogura (✉) · T. Nishimura · J. Tanida
Graduate School of Information Science and Technology, Osaka University, 1-5 Yamadaoka, Suita 565-0871, Osaka, Japan
e-mail: ogura@ist.osaka-u.ac.jp

T. Nishimura
e-mail: t-nishimura@sahs.med.osaka-u.ac.jp

J. Tanida
e-mail: tanida@ist.osaka-u.ac.jp

H. Yamamoto
Department of Optical Science and Technology,The University of Tokushima, 2-1 Minamijyousanjima-cho, Tokushima 770-8506, Japan
e-mail: yamamoto@opt.tokushima-u.ac.jp

K. Yamada
Graduate School of Medicine, Osaka University, 1-7 Yamadaoka, Suita 565-0871, Osaka, Japan
e-mail: k-yamada@sahs.med.osaka-u.ac.jp

M. Naruse (ed.), *Nanophotonic Information Physics*,
Nano-Optics and Nanophotonics, DOI: 10.1007/978-3-642-40224-1_4,

scale, and the knowledge obtained is useful for potential medical or technological applications [1, 2]. A living organism is a physical system composed of many types of matter, and it can also be considered as a sophisticated information system in which the molecules work as the information carriers. Thus, an information system capable of dealing both with matter as real objects and with the information associated with the matter is useful for obtaining valuable findings from the living organism or controlling it in an effective manner.

Processors that work in a molecular environment and deal with the information that originates from bio-molecules such as DNA, ribonucleic acid (RNA) and proteins are expected to provide an innovative methodology for analysis and control of the behavior of these bio-molecules. To realize such processors, the appropriate implementation size is essential. The size should be comparable to the size of molecules to be able to handle them directly in a molecular environment. We refer to such a small information processing apparatus with the features described above as a nano-processor.

DNA has drawn attention as a nanoscale material because of its superior features, such as Watson Crick complementarity, diversity of base sequences, and its capability for recognizing a variety of molecules [3]. For example, the self-assembly of DNA is a powerful method that can be used to fabricate two or three dimensional nanoscale structures [4–6]. The method is applicable to the arrangement of various materials with nanometer-scale precision; it is possible to form arrays of ligands or proteins, and nanoscale sensor processors based on optical resonance energy transfer [7, 8]. A variety of DNA-based nanomachines have also been demonstrated [9–11]. The features of DNA are also useful for molecular information processing. DNA computing is a promising methodology for realization of nano-processors that deal with both molecular information and real matter simultaneously. Since Adleman demonstrated the potential capabilities of DNA computing by solving a seven-city Hamiltonian path problem using DNA [12], many methods based on DNA computing have been proposed and demonstrated. Good examples of these methods include molecular automata using restriction enzymes [13] or deoxyribozymes [14], digital molecular circuits using strand displacement reactions [15], large-scale circuits using seesaw gates [16], molecular realization of a cellular automaton based on DNA self-assembly [17], and a bio-computing platform using DNAzymes [18]. Although information processing is achievable on the basis of the autonomous behavior in the DNA reactions, it usually requires complex design and precise control of the DNA reactions.

Light is another useful information carrier. Information photonics is a paradigm for the manipulation of information by the effective use of light as the information carrier. Information photonics often uses electronics, biotechnology, mechanics, and other technologies to achieve the required functionalities. Numerous interesting techniques and systems have been constructed [19], and the achievements in information photonics research are expected to be applied to the development of nanoscale information systems. However, the diffraction limit of light, by which the resolution of the light is typically restricted to around the sub-micron level for visible light, often prevents the straightforward use of light at the nanoscale. However, there are many

different types of light-matter interactions. By using these interactions, light becomes applicable to nanoscale science and technology.

By combining the ideas of DNA computing and photonics based on the effective use of light-matter interactions, a novel class of nano-processors is anticipated. For this purpose, we are studying a photonic DNA nano-processor with the functions of sensing molecular information, processing this information, and then actuating a physical action as an output [20, 21]. This is a new concept for measurement and control of a molecular system by cooperative use of DNA as the material for construction of the system and light as the interfacing carrier between the molecular system and the macro-world.

In this chapter, recent research achievements in the photonic DNA nano-processor field are described. We show the features of the photonic DNA nano-processor that acts as a mediator and performs an intermediate role between a molecular system and the macro-world. A light-activatable nano-processor and DNA scaffold logic are introduced as implementation techniques, and their properties are described.

4.2 Photonic DNA Nano-Processor

4.2.1 Concept

Photonic DNA nano-processors are nanoscale information-processing instruments that work in wet environments, and they are expected to be applied to, for example, bio-molecular systems in living organisms. The concept of the photonic DNA nano-processor is illustrated in Fig. 4.1. Photonic DNA nano-processors consist of DNA strands with different sequences, and the implementation size can therefore be of the order of nanometers. Ideally, photonic DNA nano-processors are capable of sensing or identifying molecular information, computing that information, and performing a physical action that depends on the results of the computation.

DNA molecules can interact with other biomolecules such as other DNAs, RNAs, and proteins. Therefore, the photonic DNA nano-processor is compatible with bio-molecular systems and is thus capable of capturing information related to the bio-molecules or indeed of controlling the bio-molecules. From this viewpoint, photonic DNA nano-processors are therefore not a straightforward downsizing of the conventional electronic processors that usually support our activities in the current information society. They provide novel functionalities, including on-site detection and action, because of their ability to access the bio-molecular systems directly. This property is important because it enables us to consider a molecular system not only as a target system to be measured or controlled by using the nano-processors, but also as an engineered system to be used for a particular purpose.

Matter that is responsive to light is incorporated into part of the DNA molecules of the photonic DNA nano-processor to construct a path for communication between the nano-processor and the macro-world via photonic signals. For example, the photonic

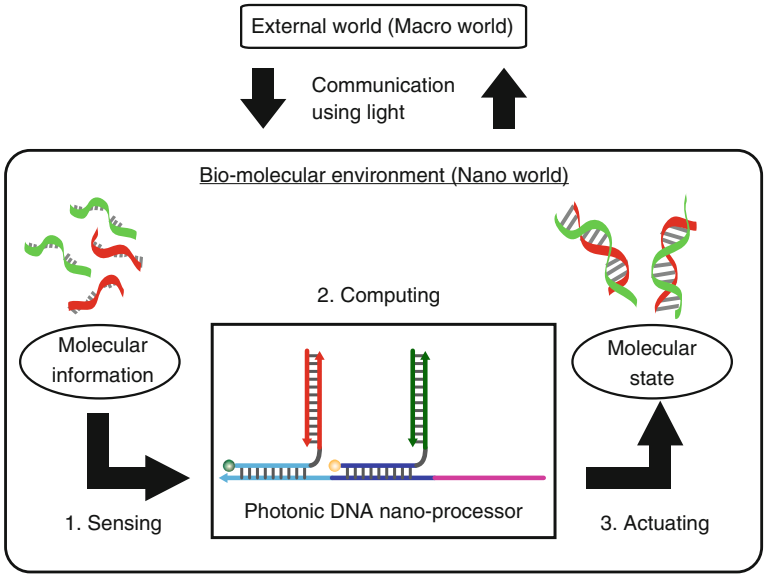

Fig. 4.1 Concept of a photonic DNA nano-processor

signals can be used to transmit control commands or external information. They can also be used to extract information from the nano-world and bring it to the macro-world. Incorporation of this photo-responsive mechanism provides a variety of functions. For example, the nano-processors can be activated at desired times. This enables stepwise progress in the processor's behavior, cooperative operation between multiple nano-processors by synchronization, and adaptive control to reflect the status of the target system. The environment of the target system is not destroyed because the photonic signals are transmitted remotely and non-invasively. In addition, the possibility of activating the nano-processors in localized volumes in parallel by distributing light into micrometer-ordered volumes is a major advantage of the use of light, because it offers position-dependent regulation of the molecular system.

4.2.2 Photonic DNA Nano-Processor as Mediator

Photonic DNA nano-processors can communicate with both the macro-world through the medium of light and the nano-world through DNA. From this viewpoint, the photonic DNA nano-processors can be considered as intelligent mediators that act as an intermediate layer between the nano-world and the macro-world.

Figure 4.2 shows a schematic diagram for acquisition of molecular information from a molecular system to the macro-world without and with a photonic DNA nano-processor as a mediator. By the conventional method (i.e. without the

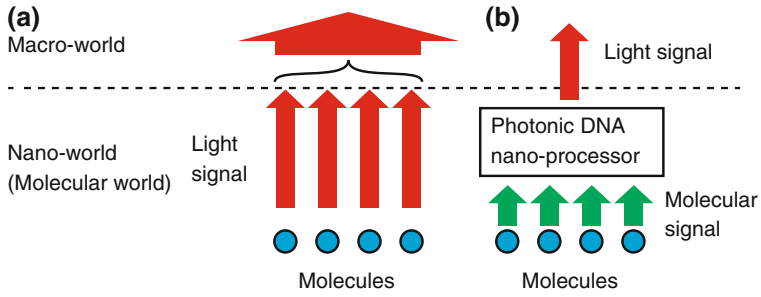

Fig. 4.2 Comparison of the information flow when molecular information is transferred from the nano-world to the macro-world, **a** without and **b** with a photonic DNA nano-processor

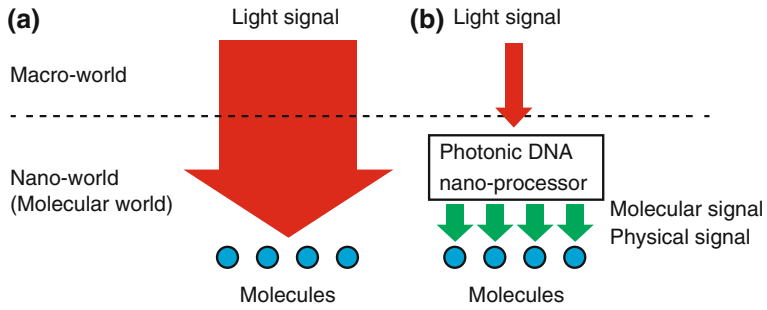

Fig. 4.3 Comparison of the information flow when a molecular system is controlled by using light, **a** without and **b** with a photonic DNA nano-processor

nano-processor), the information related to individual molecules is transferred in a straightforward way, so that a wide information bandwidth is required (Fig. 4.2a). For example, if the resolution of the imaging system is not high enough, i.e., the information bandwidth is not large enough, then the molecular information can become unexpectedly confused. In contrast, as shown in Fig. 4.2b, by using the photonic DNA nano-processor, preprocessing of the molecular information can be performed at the nanoscale to modify the information into the desired form. Logical operations and correlation operations are good examples of the preprocessing steps that can effectively suppress the amount of information. Suppression of the information at the nanoscale leads to a relaxation of the performance requirements of the apparatus used to acquire the necessary information.

Figure 4.3 shows a comparison of the methods for controlling the molecules using light. By the conventional method (Fig. 4.3a), the flexibility in the manipulation of molecules using light is restricted by the scale gap between the molecules and the light. This means that it is difficult to control individual molecules independently within the size of the light distribution. Also, direct manipulation of the molecules requires interaction between the light and the target molecules themselves. However, as shown in Fig. 4.3b, the use of a photonic DNA nano-processor offers a way to

manipulate molecules that are unresponsive to light. By using light as the trigger of the photonic DNA nano-processor, simple photonic signaling to the molecular system induces well-regulated behavior based on the capabilities of the DNA in autonomous reactions. This can be considered, from the information viewpoint, as a small amount of information carried by the light being expanded into sufficient information to control the molecular system by the photonic DNA nano-processor. Thus, despite the simplicity of the signaling, the complex behavior of the molecules can be controlled based on the autonomous reactions.

4.2.3 Types of Light Usage

The photonic DNA nano-processor has sensing, computing, and actuation functions, and photonics-based techniques can be used in these individual functions. We have considered two types of light usage in the photonic DNA nano-processor, as shown in Fig. 4.4. Light is used for activation control of the sensing function in usage type (i). In contrast, a photonic process, nanoscale photonic signal transmission, is applied to achieve the computing function in usage type (ii).

In usage type (i), the final structure of the photonic DNA nano-processor is constructed in the preliminary stage by self-assembly of DNA molecules, and then it is placed into the molecular environment. The activation of the sensing function of the nano-processor is controlled using a light signal through the response of photoresponsive molecules equipped as part of the nano-processor. This scheme offers control of the nano-processor in a specified volume of micrometer-order at the desired times because generation of arbitrary spatio-temporal patterns of the controlling light is possible. Computation is performed based on the autonomous behavior of the DNA after activation of the sensing process using the light. This photonic control ability is applicable to a variety of computation schemes based on DNA computing. It will be possible to select the function to be activated by using multiple wavelengths for the control light.

In usage type (ii), elemental DNA molecules acting as the building blocks of a photonic DNA nano-processor are inserted into a molecular system. Self-assembly of the elemental DNA molecules is used as a part of the computation process. Photoresponsive molecules are attached to some of the elemental DNA molecules, and the state of the target molecular system is encoded into the arrangement of the photoresponsive molecules. Photonic signal transmission is used to assess the molecular environment. Based on this type of usage, large-scale and high-throughput processing can be achieved, because simple DNA reactions can be used and the process proceeds in parallel by replacing the DNA reactions into a photonic process as part of the computation.

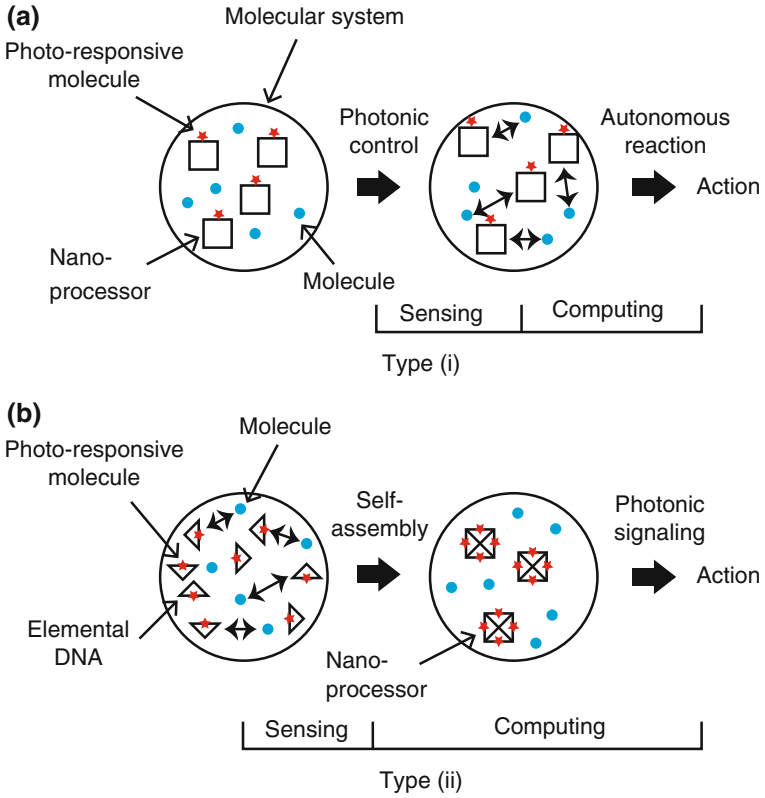

Fig. 4.4 Two types of light usage. **a** Type (*i*): the light is used to activate the sensing function. **b** Type (*ii*): a photonic signal is used as part of the computation process

4.3 Light-Activatable DNA Nano-Processor

4.3.1 Activation of Sensing Function Using Light

A photonic DNA nano-processor with a light-activatable sensing function was constructed as a prototype of usage type (i). The light-activatable DNA nano-processor senses two particular sequences of the DNA strands, decides whether the sensed DNA contains a target sequence, and transforms as an action. One distinctive feature is that the sensing function can be activated or inactivated by using photonic signals. For this purpose, the DNA tethered with a photo-isomerization molecule, azobenzene, was used [22]. The azobenzene-tethered DNA binds with its complementary DNA to form a double-stranded DNA when the azobenzene is in the trans-form upon visible light irradiation. This double-stranded DNA is separated into single-stranded

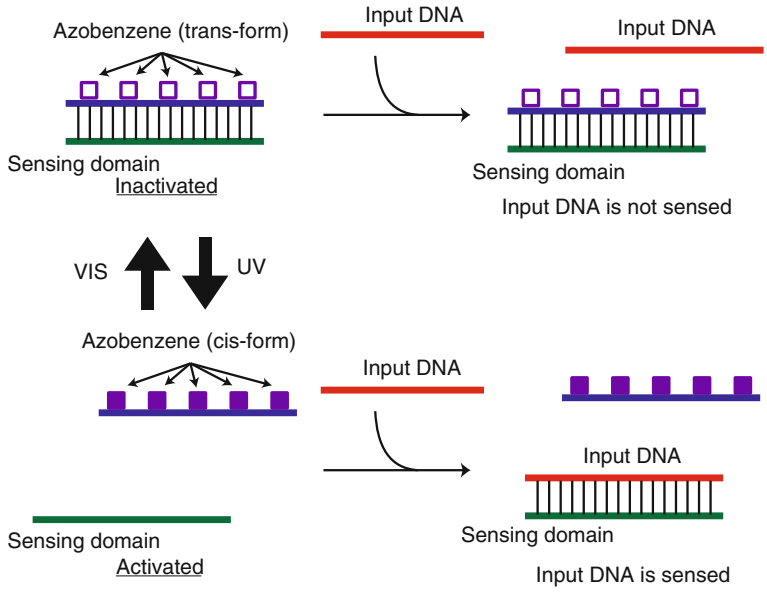

Fig. 4.5 Method for controlling the activation of the sensing function. Upon UV light irradiation, the sensor is activated, and upon visible light irradiation, the sensor is inactivated

DNAs when the azobenzene is in the cis-form upon ultraviolet (UV) light irradiation. This property enables the activation of the sensing function and also its inactivation.

Figure 4.5 shows the basic activation control scheme. The sensing domain binds with its complementary sequence with azobenzene upon visible light irradiation. In this case, the sensing function is inactivated, because the sensing domain is shielded to prevent it from binding with other DNA fragments. However, the sensing domain is exposed upon UV light irradiation. As a result, the sensing function is activated because the sensing domain is ready to bind with other DNA fragments. In this case, the input DNA can be sensed.

4.3.2 Scheme

The behavior of the light-activatable nano-processor is shown in Fig. 4.6. The nano-processor forms a tweezer-like structure with two hairpin DNAs which incorporate azobenzene molecules for photonic control. DNA tweezers were first demonstrated by Yurke et al. [9] as a DNA nanomachine by using a strand displacement reaction. Photonically-controlled DNA tweezers have also been demonstrated as a DNA nanomachine [23, 24]. However, the nano-processor with activation control is substantially different from the DNA tweezers described above.

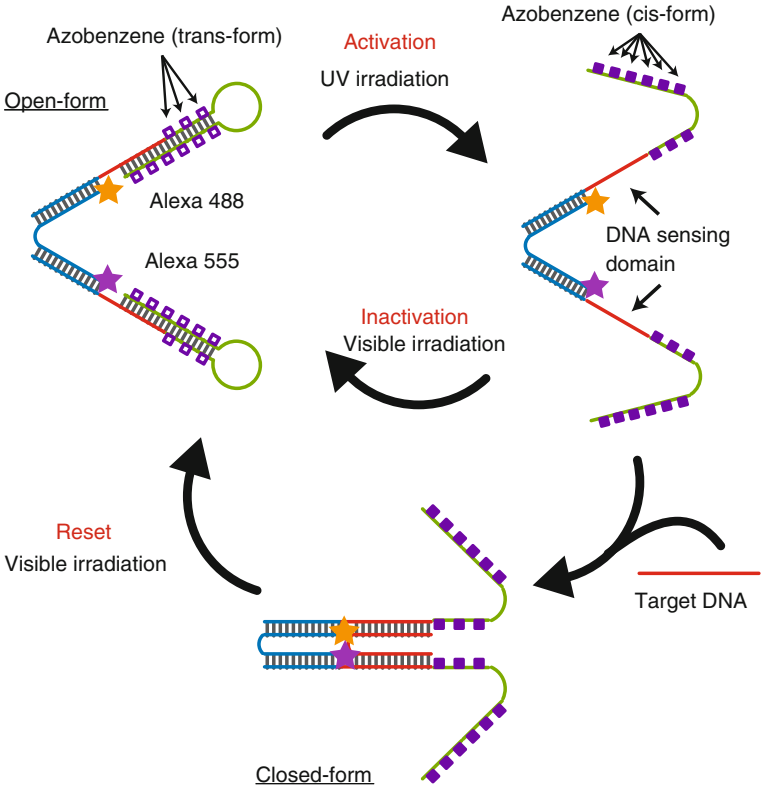

Fig. 4.6 Reaction scheme of light-activatable DNA nano-processor

In the sensing function, the nano-processor binds to a particular DNA fragment. The hairpin DNAs located at the individual edges contain sensing domains with sequences that are different from each other. This means that the individual hairpin DNAs can sense sequences independently. The hairpin DNAs open upon UV light irradiation, and the sensing domains are exposed to start the sensing process. The hairpin DNAs close upon visible light irradiation to inactivate the sensing function.

In the computing function, the nano-processor judges whether a DNA fragment binds to both sensing domains on the individual arms of the tweezers. Then, for the actuating function, the nano-processor closes its structure or maintains the open form, depending on the result. If the sensed DNA fragment contains the target sequence, then it is captured by both arms. This means that "the result is YES," and the nano-processor assumes the closed form. However, if the fragment does not contain the target sequence, it is captured by only one or neither arm. This means that "the result is NO," and the structure maintains the open form. Note that the nano-processor changes from the open form to the closed form by binding with the target DNA

only during the periods of activation. During the periods of inactivation, the nano-processor does not change its form, regardless of the existence of the target DNA.

Another interesting function is the possibility of reset. By irradiation with visible light, the target DNA captured during the period of activation is released because the hairpin DNAs close, and then the nano-processor transits to the open form (the initial form). Photo-activation of DNA probes was previously demonstrated by Wang et al. [25], but repeated sensing was impossible because of the lack of a reset function. The reset function enables the photonic DNA nano-processors to be used repeatedly.

4.3.3 Experiments

Before demonstration of the entire nano-processor, we investigated the behavior of a sensor consisting of two hairpin DNAs tethered with azobenzenes to clarify the properties of the sensing function [26]. The scheme and the DNA sequences used are shown in Fig. 4.7. One of the fluorescent dyes, 6-FAM (excitation/emission: 494/517 nm) and TAMRA (excitation/emission: 565/580 nm), is attached to each of the individual hairpin DNAs. These dyes form a fluorescence resonance energy transfer (FRET) pair. Under UV light irradiation, sensing is activated because the sensing domains are exposed as described in Sect. 4.3.1. When the target DNA exists during the period of activation, the target binds to both hairpin DNAs, and the fluorescent

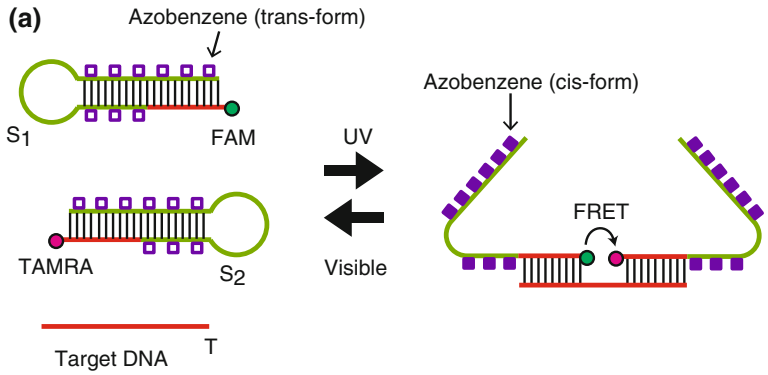

(b)

S_1: 5' FAM-ATCTGAACTAACGCTxTTxAAxGATCTCTxCTxTAxAAxGCxG--TxTAxGTxTCA 3'

S_2: 5' CACxGTxACxATxGCTxTTxAAxGATCTCTxCTxTAxAAxGCATGTAC--GTGCTA-TAMRA 3'

T: 5' CGTTAGTTCAGATATCATAGCACGTACATG 3'

Fig. 4.7 **a** Scheme of the light-activatable sensor using two hairpin DNAs with azobenzene. **b** Sequences and modifications of the DNA strands used. The symbol x indicates the position of the azobenzene

dyes of the FRET pair are placed closely together, as shown in Fig. 4.7. In this case, the FRET occurs. By irradiation with visible light, the sensor returns to its initial form to be reset. The sensing results can be obtained by measuring the fluorescence signals.

We used a spectrofluorometer (JASCO CORPORATION, FP-6200) for switching activation/inactivation and for measurement of the fluorescence intensity. A xenon lamp was used as the light source. The wavelengths of the light used were 340 ± 10 nm (5 mW/cm^2) for activation and 440 ± 10 nm (7 mW/cm^2) for inactivation. The 494 nm wavelength light was used for excitation of FAM, and its fluorescence intensity was measured at 517 nm (emission wavelength of FAM). Irradiations for activation and inactivation were performed at 80 °C for two minutes, because the efficiency of the photoisomerization of azobenzene between the cis-form and the trans-form is high at high temperatures. The fluorescence intensities were measured at 25 °C.

The first experiment was performed to measure the dependence of the FRET ratio on the static concentration of the target DNA. The FRET ratio is defined as $1 - F/F_0$, where F is the fluorescence intensity of the donor of the FRET pair after sensing and F_0 is that before the sensing process. Figure 4.8 shows the relationship between the FRET ratio after activation and the concentration of the target DNA when the concentration at the sensor is 0.5 μM. The FRET ratio is approximately proportional to the target concentration. This result indicates that it is possible for this sensor to measure the target concentration.

The second experiment was conducted to investigate the dependence on the concentration of the target DNA when the concentration varied. Figure 4.9 shows the changes in the FRET ratio when the target DNA increased or decreased.

The target concentration was changed from 0.1 μM to 0.3 μM by adding the target DNA in the experiment of Fig. 4.9a, and it was changed from 0.4 μM to 0.2 μM by adding 0.2 μM of the complimentary DNA of the target shown in the experiment of Fig. 4.9b. The sensor concentration was 0.5 μM. These results demonstrate that the FRET ratio changed according to the concentration at the activation time. The FRET ratio values are almost in agreement with the results of Fig. 4.8. The sensor is suitable for reporting the concentration of the target DNA at the desired timings, regardless of the concentration at the previous measurement.

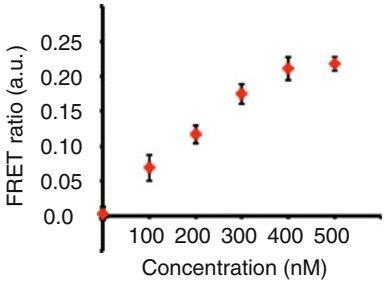

Fig. 4.8 Dependence of the FRET ratio on the input DNA concentration

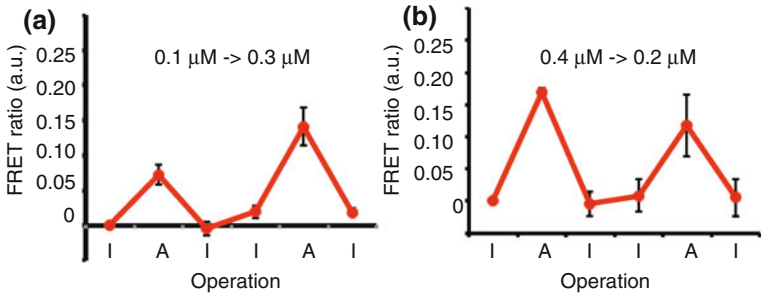

Fig. 4.9 The FRET ratio measured when the input DNA concentration changes. **a** The input DNA increases from 0.1 to 0.3 μM. **b** The input DNA decreases from 0.4 to 0.2 μM. A: Activated (UV light), I: Inactivated (Visible light)

Next, we constructed the light-activatable nano-processor shown in Fig. 4.6 to demonstrate its function. One of the pair of fluorescent dyes, Alexa 488 (excitation/emission: 495/520 nm) and Alexa 555 (excitation/emission: 550/570 nm), was attached to each of the nano-processor's arms to act as a donor and an acceptor of a FRET pair to report on the nano-processor's form. The fluorescence intensity of Alexa 488 is high when the nano-processor is in the open form, but the intensity becomes low when the nano-processor is in the closed form. The sequences of and modifications for the light-activatable nano-processor, which consists of three DNA strands, are summarized in Fig. 4.10. The FRET ratio was measured under three different conditions as follows: (i) a solution containing 5-μM target DNA and the 1-μM nano-processor was activated and inactivated three times in succession; (ii) the solution containing only the 1-μM nano-processor (no target DNA) was activated and inactivated once, (iii) the solution containing 5-μM target DNA and the 1-μM nano-processor was left without any irradiation. The irradiation processes for activation and inactivation were performed at 60 °C to maintain the structures of the light-activatable nano-processors. The fluorescence intensities were measured at 37 °C.

The FRET ratio measured after the individual operations is shown in Fig. 4.11. The FRET ratio increased upon UV light irradiation (activation) and decreased

Hairpin 1: 5' Alexa488-ACAGTTTGTCCTGGGCATCAGCTGCCGTGCTTTGCG-
-Alexa555 3'
Hairpin 2: 5' GCCCAGGACAAACTGTCTACTACCTCACxCTxAGxCTCTTCTG-
-CxTAxGGxTGxAGxGTxAG 3'
Hinge: 5' GTxATxGGxTTxCGxTTxAGTCTTCTCxTAxACxGAACCATACAACC-
-GCAAAGCACGGCAGC 3'
Target: 5' TGAGGTAGTAGGTTGTATGGTT 3'

Fig. 4.10 Sequences and modifications for the light-activatable nano-processor. The symbol x indicates the position of the azobenzene

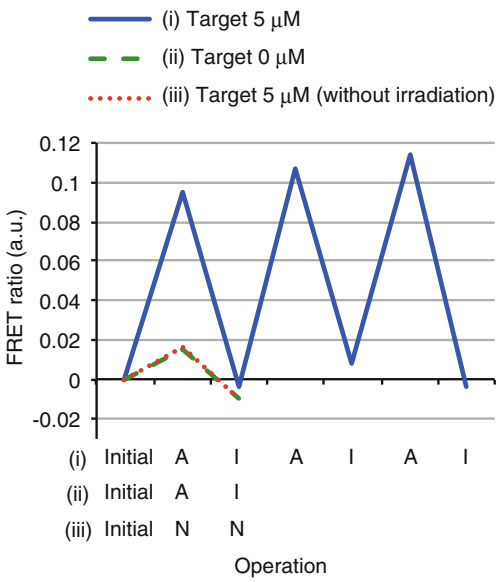

Fig. 4.11 Variance of the FRET ratio during repeated activation and inactivation operations of light-activatable DNA nano-processor. *A* Activated (UV light), *I* Inactivated (visible light), *N* Neutral (no light)

upon visible light irradiation (inactivation) for condition (i). However, the FRET ratio changed little for conditions (ii) and (iii). This result indicates that activation/inactivation of the sensing function is controlled via the external photonic signals, and the nano-processor transforms under the existence of the target DNA during the activation periods. Note that the measured FRET ratios during the activation periods are almost the same value for any number of repetitions. This suggests that stable behavior is obtained during the repetition process. Also, the FRET ratio decreased to approximately 0 after inactivation. This behavior is considered to be the result of the nano-processor releasing the previously detected DNA and returning to its initial form. The experimental results demonstrate that the nano-processor transforms, depending on whether or not the target DNA exists, and that it can be reset to work repeatedly by synchronization of the activation control using light.

4.4 DNA Scaffold Logic

4.4.1 Fundamental Scheme of Logic Operation

The DNA scaffold logic [27], which we have proposed, is a typical example of type (ii) usage of the light. The nano-processor based on DNA scaffold logic is capable of executing a logical operation with the DNA inputs and producing an output as a fluorescence signal. In this scheme, a DNA scaffold, on which the photonic process is performed, is prepared. The DNA scaffold sequence depends on the given logic

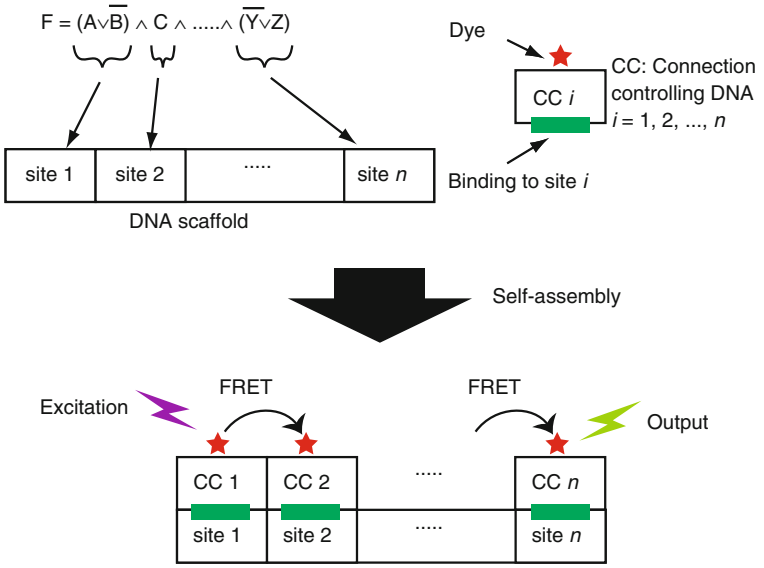

Fig. 4.12 Logic operation by DNA scaffold logic. Fluorescent dyes are placed on a scaffold according to the input DNA. The result is reported by the FRET cascades

function. Connection-controlling DNAs with a fluorescent dye are also used. The connection-controlling DNAs interact with the input DNAs, and place the fluorescent dye on the DNA scaffold or remove it from the scaffold. As a result, the target molecular system status is encoded into an arrangement of fluorescent dyes on the DNA scaffold. This process is performed based on the self-assembly of DNA.

To explain the process in more detail, let us consider that a given logic function is in the conjunctive normal form with n clauses, as shown in Fig. 4.12. A single-stranded DNA is used as a DNA scaffold. The DNA scaffold contains n sites (site 1, site 2,..., site n), and the different connection-controlling DNAs can bind at individual sites. The individual sites correspond to the different clauses. A connection-controlling DNA with a fluorescent dye binds to a particular site when the corresponding clause is TRUE for the input DNA. If the fluorescent dyes bind to site i and site $i + 1$, the energy of the excited dye on site i then transfers to another dye on site $i + 1$. Thus, a FRET path from site 1 to site n is constructed on the scaffold, but only if the input satisfies all of the clauses; i.e. that the given logic function is TRUE. As a result, the dye on site n produces a fluorescent signal by excitation of the dye on site 1. If one or more clauses are not satisfied, then the FRET path is broken on the way from site 1 to site n. As a result, the dye on site n produces no fluorescent signal to show that the logic function is FALSE.

4.4.2 Features

The DNA scaffold logic has distinctive features as nano-processors. Figure 4.13 shows a comparison between the conventional DNA logic and DNA scaffold logic. In conventional DNA logic, a number of the DNA complexes are used as computing elements, and cascaded reactions between the elements via molecular signals are used for computation. Thus, the computation generally proceeds in a sequential manner. In contrast, in DNA scaffold logic, the molecular signals are converted to an arrangement of fluorescent dyes, and part of the computation is performed by FRET signaling on the single DNA scaffolds. The FRET signaling path is constructed by placing connection-controlling DNAs with fluorescent dyes at different sites on the scaffold. The placement process proceeds in parallel and independently. This scheme no longer requires the cascaded reactions via the molecular signal. Therefore, the operation is fast, and complicated logic operations can be executed with a few additional time periods for the operation. Self-assembly is used to arrange the fluorescent dyes as part of the computation, and therefore the operation is expected to be powerful. Also, the error caused by the DNA reaction does not propagate to subsequent reactions because the reactions are designed in an independent manner. Signal transmission is performed using a FRET cascade, which is not a diffusion process of molecules, and the signal transmission efficiency is high.

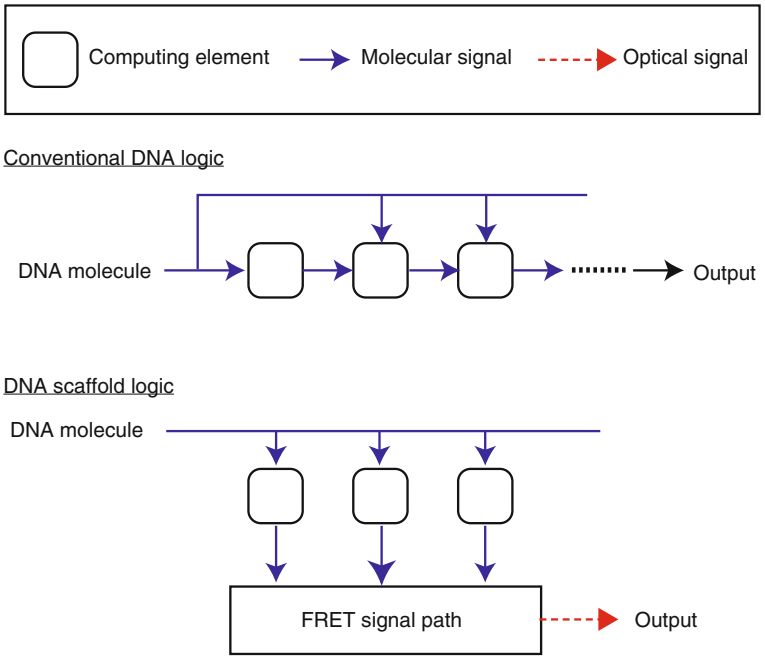

Fig. 4.13 Comparison of logic operations by conventional DNA logic and by DNA scaffold logic

4.4.3 Experiments

We designed two reactions for connection-controlling DNAs to arrange fluorescent dyes on a DNA scaffold. The first is a reaction using a connecting DNA to realize the function of a YES gate. The second is a reaction using a disconnecting DNA to realize the function of a NOT gate. The schemes of these reactions are shown in Fig. 4.14. For the YES gate, a hairpin DNA with a fluorescent dye is used as the connecting DNA. When an input DNA binds to the connecting DNA through a strand displacement reaction, the domain to be bound to the scaffold is exposed, and then the connecting DNA binds to the scaffold to carry the dye on the scaffold. For the NOT gate, a disconnecting DNA with a dye is bound on the scaffold; i.e. the fluorescent dye is arranged on the scaffold previously. When an input DNA exists, it binds to the disconnecting DNA and removes the dye from the scaffold. In contrast, the dye remains on the scaffold when the input DNA does not exist. Note that a variety of sequences can be used as the sequence for the domain for recognition of the input DNA or for binding to the scaffold. These schemes are therefore useful for dealing with large numbers of inputs and complicated logic functions.

Several logic functions were tested to demonstrate DNA scaffold logic. Figure 4.15a shows the scheme and the results of the logic function $I_1 \wedge I_2$ used to demonstrate the AND operation. The sequences and modifications that were used

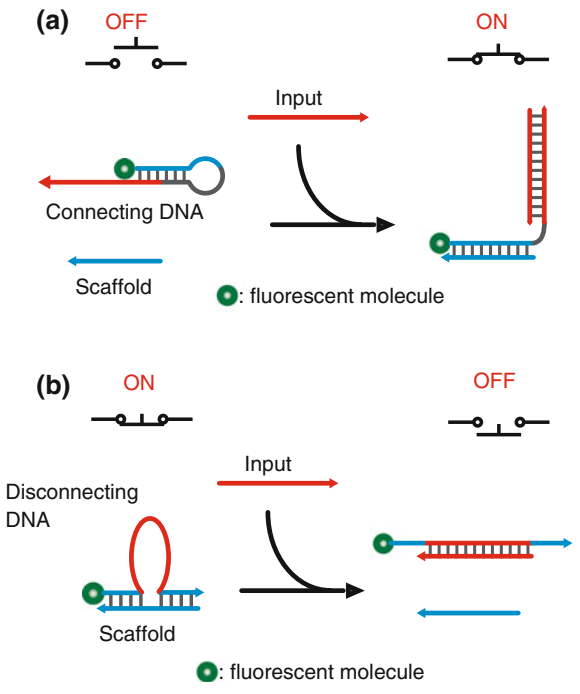

Fig. 4.14 Reaction schemes for **a** a connecting DNA and **b** a disconnecting DNA. When using the connecting DNA, the dye is placed on the scaffold when an input DNA exists. When using the disconnecting DNA, the dye is put on the scaffold when the input DNA does not exist

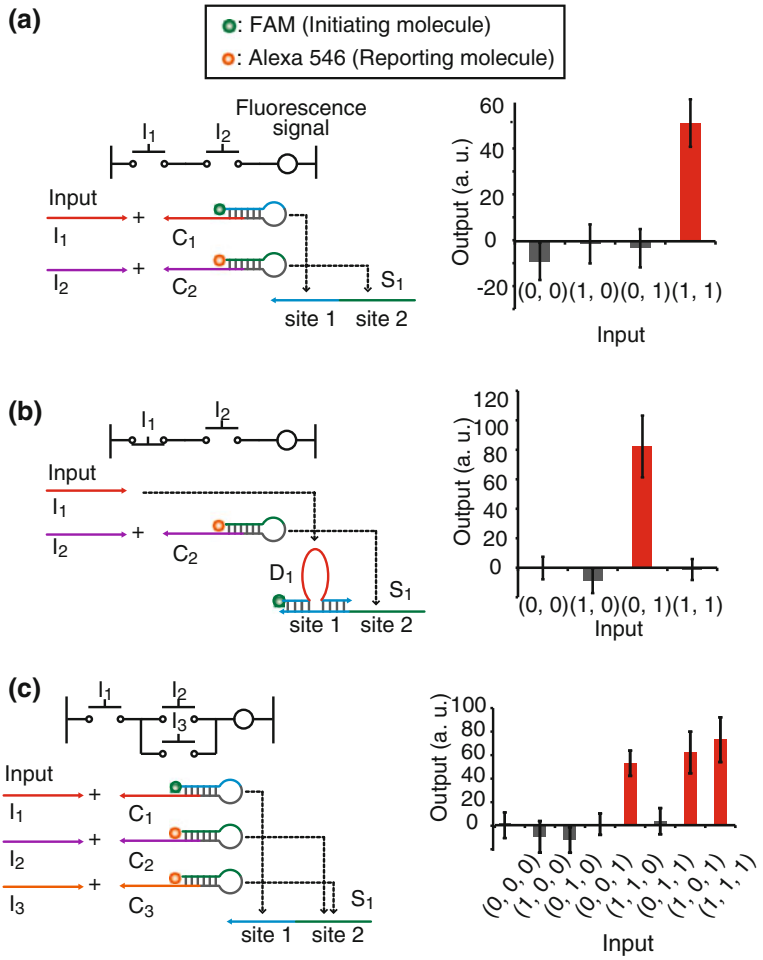

Fig. 4.15 Schemes and operation results for possible combinations of the inputs. **a** $I_1 \wedge I_2$, **b** $\neg I_1 \wedge I_2$, and **c** $I_1 \wedge (I_2 \vee I_3)$

are shown in Fig. 4.16. Two sites were formed on the scaffold. The individual sites can bind with the connecting DNAs for inputs I_1 and I_2. FAM and Alexa 546 (excitation/emission: 556/573 nm) were used as the FRET pair. When the two inputs I_1 and I_2 both exist, then the FRET path from FAM to Alexa 546 can be constructed on the scaffold. The concentrations of the input DNAs were 0 μM and 2 μM for the input values "0" and "1," respectively. The concentrations of the other components were 0.4 μM. The results for the possible combinations of the values of I_1 and I_2 are shown on the right side of Fig. 4.15a. The output signal is defined as the fluorescence intensity at the emission peak wavelength of the reporting dye when measured after adding the input DNAs, but minus the intensity measured before the addition.

S_1: 5' CATCGGGTGAGCGCTTCGGCAGAGCG 3'
S_2: 5' GCAACTATGAGCGCATCGGGTGAGCGCTTCGGCAGAGCG 3'
C_1: 5' FAM-CGCTCTGCCGAAGGCAGAGCGCCACTTACAA 3'
C_2: 5' Alexa546-CGCTCACCCGATGGGTGAGCGCTCAAGGATT 3'
C_3: 5' Alexa546-CGCTCACCCGATGGGTGAGCGAGGTAGTTGT 3'
C_4: 5' Alexa594-CGCTCATAGTTGCTATGAGCGAGGTAGTTGT 3'
D_1: 5' FAM-CGCTCTACCACTTACAAAGCCGAAG 3'
I_1: 5' TTGTAAGTGGCGCTC 3'
I_2: 5' AATCCTTGAGCGCTC 3'
I_3: 5' ACAACTACCTCGCTC 3'

Fig. 4.16 Sequences and modifications of the DNA strands used

The operational results show that a high fluorescence signal is obtained only when $(I_1, I_2) = (1, 1)$. This result indicates that the connecting DNAs work well and that the AND operation is executed successfully.

Figure 4.15b shows the scheme and the results of the logic function $\neg I_1 \wedge I_2$ used to demonstrate NOT operation. A disconnecting DNA which binds to site 1 was used for input I_1, and a connecting DNA which binds to site 2 was used for input I_2. The operation results show that a high output signal is obtained only for $(I_1, I_2) = (0, 1)$. The results demonstrate that operations including NOT are executed.

Figure 4.15c shows the scheme and the result of the logic function $I_1 \wedge (I_2 \vee I_3)$ used to demonstrate OR operation. For execution of the OR operation, the same fluorescent dye, Alexa 546, is assigned to inputs I_2 and I_3. The connecting DNAs for inputs I_2 and I_3 are different, but both DNAs can bind to site 2. As a result of this design, Alexa 546 is placed on site 2 when input I_2 or I_3 is "1". The result shows that high output signals are obtained for inputs of (1, 1, 0), (1, 0, 1), and (1, 1, 1). OR operation is therefore achievable based on the above design.

To demonstrate logic with more than 2 clauses, the logic function $I_1 \wedge I_2 \wedge I_3$ was executed. Figure 4.17 shows the scheme and the results. Three sites were formed on the DNA scaffold, and different connecting DNAs with three different fluorescent dyes, FAM, Alexa 546, and Alexa 594 (excitation/emission: 590/619 nm), were used. A high output signal was obtained only when $(I_1, I_2, I_3) = (1, 1, 1)$. This result demonstrates that the fluorescent dyes are arranged adequately according to the input and the logical operation with three clauses is executed successfully. The output signal is not low enough for inputs of (0, 1, 1), (1, 0, 1), and (1, 1, 0). Possible reasons for this are direct excitation of the second dye (Alexa 546) and FRET from the first dye (FAM) to the third (Alexa 594).

4.4.4 Analysis of Properties

Some properties of DNA scaffold logic were investigated by numerical analysis of the reactions. Let us consider the reactions between the input DNAs (I), the connecting

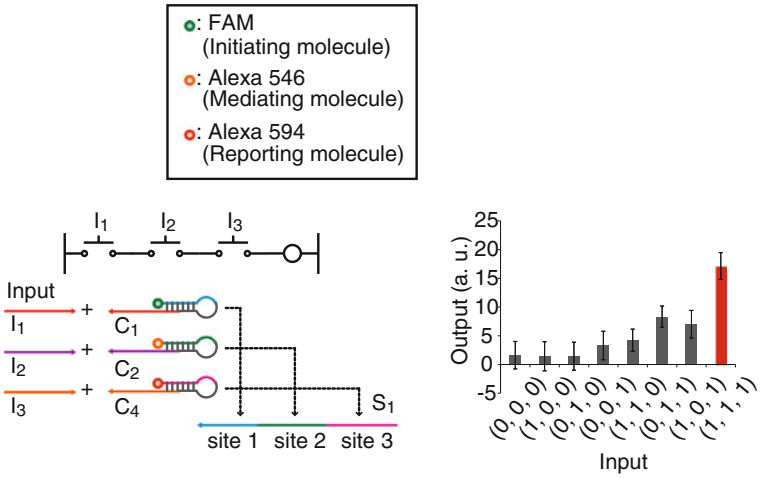

Fig. 4.17 The scheme and results for the logic function $I_1 \wedge I_2 \wedge I_3$

DNAs (C), and the DNA scaffolds(S). The reactions can be represented by chemical equations as shown in Fig. 4.18. Here, IC denotes a complex of DNAs I and C, while ICS denotes a complex of DNAs I, C, and S. k_1 is the reaction rate constant of the first reaction, and k_2 and k_3 are the reaction rate constants of the second reaction. The reaction rate equations are written as follows:

$$-\frac{d[I]_t}{dt} = k_1[I]_t[C]_t, \tag{4.1}$$

$$-\frac{d[C]_t}{dt} = k_1[I]_t[C]_t, \tag{4.2}$$

$$\frac{d[IC]_t}{dt} = k_1[I]_t[C]_t - k_2[IC]_t[S]_t + k_3[ICS]_t, \tag{4.3}$$

$$-\frac{d[S]_t}{dt} = k_2[IC]_t[S]_t - k_3[ICS]_t, \tag{4.4}$$

$$\frac{d[ICS]_t}{dt} = k_2[IC]_t[S]_t - k_3[ICS]_t, \tag{4.5}$$

$$[I]_0 = [I]_t + [IC]_t + [ICS]_t, \tag{4.6}$$

$$[C]_0 = [C]_t + [IC]_t + [ICS]_t, \tag{4.7}$$

Fig. 4.18 Chemical equations of the reactions between the input DNAs (I), the connecting DNAs (C), and the DNA scaffolds (S)

$$I + C \xrightarrow{k_1} IC$$

$$IC + S \underset{k_3}{\overset{k_2}{\rightleftarrows}} ICS$$

$$[S]_0 = [S]_t + [ICS]_t, \tag{4.8}$$

$$[IC]_0 = 0, \tag{4.9}$$

$$[ICS]_0 = 0. \tag{4.10}$$

Here $[\cdot]_t$ represents the concentration at time t, and $[\cdot]_0$ represents the initial concentration. From these equations, a single-variable differential equation on $[ICS]_t$ is derived as

$$\begin{aligned}\frac{[ICS]_t}{dt} &= \frac{k_2[I]_0[C]_0[S]_0(1-\exp\{([I]_0-[C]_0)k_1t\})}{[C]_0-[I]_0\exp\{([I]_0-[C]_0)k_1t\}} \\ &\quad -\left(k_2[S]_0+\frac{k_2[I]_0[C]_0(1-\exp\{([I]_0-[C]_0)k_1t\}}{[C]_0-[I]_0\exp\{([I]_0-[C]_0)k_1t\}}+k_3\right)[ICS]_t \\ &\quad +k_2[ICS]_t^2 \quad (\text{for } [I]_0 \neq [C]_0), \end{aligned} \tag{4.11}$$

$$\begin{aligned}\frac{d[ICS]_t}{dt} &= \frac{k_2[C]_0^2[S]_0k_1t}{[C]_0k_1t+1}-\left(k_2[S]_0+\frac{k_2[C]_02k_1t}{[C]_0k_1t+1}+k_3\right)[ICS]_t \\ &\quad +k_2[ICS]_t^2 \quad (\text{for } [I]_0 = [C]_0). \end{aligned} \tag{4.12}$$

This equation was solved numerically using the fourth-order Runge-Kutta method [28]. In the calculation, we simply assume that $k_1 = 3.4 \times 10^6\ \mathrm{M^{-1}s^{-1}}$, $k_2 = 7.2 \times 10^4\ \mathrm{M^{-1}s^{-1}}$, and $k_3 = 4.8 \times 10^{-4}\ \mathrm{s^{-1}}$. These were values estimated experimentally.

Figure 4.19 shows the dependence of $[ICS]_t$ on $[I]_0$, where $[C]_0 = 1.0\ \mu\mathrm{M}$, $[S]_0 = 1.0\ \mu\mathrm{M}$. $[ICS]_t$ indicates the concentration of the scaffold on which a fluorescent dye carried by DNA C is placed. At any time, $[ICS]_t$ is approximately proportional to $[I]_0$ when $[I]_0 < 1.0\,\mu\mathrm{M}$. Therefore, the ratio of the fluorescent dyes on the scaffold depends on the concentration of the input DNA. However, $[ICS]_t$ is almost constant when $[I]_0 \geq 1.0\ \mu\mathrm{M}$. This indicates the robustness of the behavior

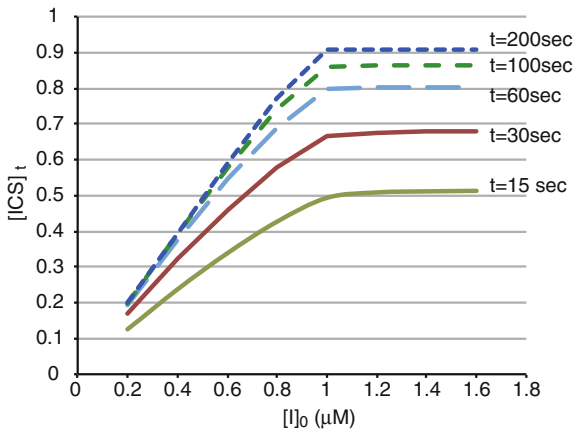

Fig. 4.19 Dependence of $[ICS]_t$ on $[I]_0$ at different times

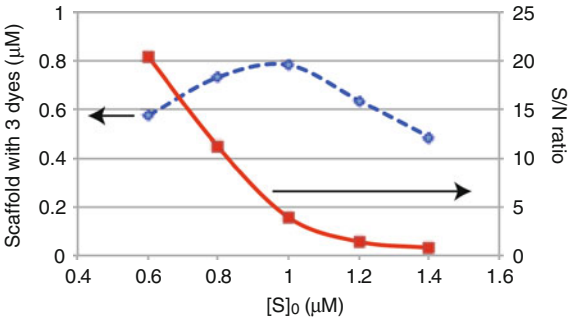

Fig. 4.20 Dependence of the amount of scaffolds with 3 fluorescence dyes (left axis) and the S/N ratio (right axis) on $[S]_0$

of $[ICS]_t$ for the variance of $[I]_0$, which is more than a value. The feature is useful for construction of digital circuits based on DNA scaffold logic.

Next, the signal to noise ratio (S/N) is estimated. When the DNA scaffold contains n sites, the ratio, $R_t(n, k)$, of the scaffold on which $k(\leq n)$ fluorescent dyes are placed is given by

$$R_t(n,k) = {}_nC_k \left(\frac{[IHS]_t}{[S]_0}\right)^k \left(1 - \frac{[IHS]_t}{[S]_0}\right)^{n-k}, \tag{4.13}$$

where ${}_nC_k$ is the k-combination from n elements. As described in Sect. 4.4.3 with regard to Fig. 4.17, when 2 out of the 3 dyes are placed on the scaffold, the reporting dye produces a measurable output signal as noise. We therefore define the S/N ratio as $R_\infty(n,n)/R_\infty(n,n-1)$. Figure 4.20 shows the dependence of the amount of scaffolds with n fluorescence dyes ($R_\infty(n,n) \times [S]_0$) and the S/N ratio on $[S]_0$ when $n = 3$, $[I]_0 = 1.0$ μM, and $[C]_0 = 1.0$ μM. The largest amount of scaffolds with 3 dyes is obtained around $[S]_0 = 1.0$ μM. Therefore, $[S]_0 = 1.0$ μM is a good choice under the conditions considered from the viewpoint of sensitivity for fluorescence detection. The S/N ratio, however, decreases with increasing $[S]_0$, which means that a smaller $[S]_0$ is better. These results indicate that the scaffold concentration should be determined carefully by considering the detector sensitivity and the acceptable S/N ratio.

4.5 Conclusions and Outlook

In this chapter, we presented the concept of the photonic DNA nano-processor and its implementation methods. This is a photonics-based approach to realize the molecular processing associated with physical processes such as sensing and actuation. In particular, we focused on the nano-processors that transform based on light-activatable sensing or that produce a FRET signal as a result of a logical operation based on molecular inputs. The basic concepts were demonstrated and some performance characteristics were then revealed by experimental and numerical analyses.

We then considered the future prospects of the photonic DNA nano-processor. We demonstrated the fundamental function of processing by the use of light-activatable nano-processors and using DNA scaffold logic. Functional extension is, however, required to realize valuable nanoscale information systems. For example, we are constructing a type of memory used in a FRET circuit [29]. The memory function is indispensable for an infinite automaton, which is more powerful than combinatorial logic. Communication among the nano-processors is also important to enhance the functionality. Along with molecular communication, broad-casting or broad-gathering using light will also be effective.

In Sect. 4.4.4, some characteristics were derived from analyses of the reactions. These findings support the issues for design of the photonic DNA nano-processors. Theoretical investigations, especially from the viewpoints of systems or information, will be useful for generation of design guidelines and for highlighting the technological issues in this field.

There are many potential applications of this technology. In particular, monitoring and regulating the activities of groups of cells is promising, because adaptive and parallel control depending on the status of the cells in question is possible based on the intermediate layer formed by the nano-processor between the nano-world and the macro-world. The photonic DNA nano-processor is expected to be a powerful tool in nanoscience fields including synthetic biology and drug delivery.

Acknowledgments This work was supported by Grants-in-Aid for Scientific Research (B) (No. 22300103) and for Scientific Research on Innovative Areas "Nanomedicine Molecular Science" (No. 2306) from the Ministry of Education, Culture, Sports, Science, and Technology of Japan.

References

1. J.K. Willmann, N. Bruggen, L.M. Dinkelborg, S.S. Gambhir, Nat. Rev. Drug Discov. **7**, 591 (2008)
2. B. Huang, H. Babcock, X. Zhuang, Cell **143**, 1047 (2010)
3. N.C. Seeman, Annu. Rev. Biochem. **79**, 65 (2010)
4. E. Winfree, F. Liu, L.A. Wenzler, N.C. Seeman, Nature **394**, 539 (1998)
5. P.W.K. Rothemund, Nature **440**, 297 (2006)
6. E.S. Andersen, M. Dong, M.M. Nielsen, K. Jahn, R. Subramani, W. Mamdouh, M.M. Golas, B. Sander, H. Stark, C.L.P. Oliveira, J.S. Pedersen, V. Birkedal, F. Besenbacher, K.V. Gothelf, J Kjems. Nature **459**, 73 (2009)
7. S.H. Park, P. Yin, Y. Liu, J.H. Reif, T.H. LaBean, H. Yan, Nano Lett. **5**, 729 (2005)
8. W. Chongchitmate, C. Dwyer, A.R. Lebeck, IEEE Micro **30**, 110 (2010)
9. B. Yurke, A.J. Turberfield, A.P. Mills Jr, F.C. Simmel, J.L. Neumann, Nature **406**, 605 (2000)
10. W.B. Sherman, N.C. Seeman, Nano Lett. **4**, 1203 (2004)
11. J. Bath, A.J. Turberfield, Nature Nanotechnol. **2**, 275 (2007)
12. L.M. Adleman, Science **266**, 1021 (1994)
13. Y. Benenson, B. Gil, U. Ben-Dor, R. Adar, E. Shapiro, Nature **429**, 423 (2004)
14. M.N. Stojanovic, D. Stefanovic, Nat. Biotechnol. **21**, 1069 (2003)
15. G. Seelig, D. Soloveichik, D.Y. Zhang, E. Winfree, Science **314**, 1585 (2006)
16. L. Qian, E. Winfree, J. Bruck, Nature **475**, 368 (2011)

17. P.W.K. Rothemund, N. Papadakis, E. Winfree, PLoS Biol. **2**, 2041 (2004)
18. J. Elbaz, O. Lioubashevski, F. Wang, F. Remacle, R.D. Levine, I. Willner, Nature Nanotech. **5**, 417 (2010)
19. P. Cheben (ed.), *Proceedings of 2011 ICO International Conference on Information Photonics (on CD-ROM)*, Ottawa, 2011.
20. T. Nishimura, Y. Ogura, K. Yamada, H. Yamamoto, J. Tanida, Proc. SPIE **8102**, 810207 (2011)
21. T. Nishimura, Y. Ogura, K. Yamda, H. Yamamoto, J. Tanida, *in Abstracts for 8th Annual Conference on Foundations of Nanoscience* (Snowbird Cliff Lodge, Snowbird, Utah, April, 2011), pp. 181–182
22. H. Asanuma, X. Liang, H. Nishioka, D. Matsunaga, M. Liu, M. Komiyama, Nat. Protocols **2**, 203 (2007)
23. X. Liang, H. Nishioka, N. Takenaka, H. Asanuma, ChemBioChem **9**, 702 (2008)
24. Y. Ogura, T. Nishimura, J. Tanida, Appl. Phys. Express **2**, 025004 (2009)
25. C. Wang, Z. Zhu, Y. Song, H. Lin, C.J. Yang, W. Tan, Chem. Commun. **47**, 5708 (2011)
26. T. Nishimura, Y. Ogura, J. Tanida, Biomed. Opt. Express **3**, 920 (2012)
27. T. Nishimura, Y. Ogura, J. Tanida, Appl. Phys. Lett. **101**, 233703 (2012)
28. W. H. Press, B. P. Flannery, S. A. Teukolsky, W. T. Vetterling, *Numerical Recipes in FORTRAN: The Art of Scientific Computing*, 2nd ed. (Cambridge, England: Cambridge University Press, 1992), pp. 704–708.
29. T. Nishimura, Y. Ogura, J. Tanida, Appl. Phys. Express **6**, 015201 (2013)